

# Earth, Planets and Space

## Comment on “Earthquake-induced prompt gravity signals identified in dense array data in Japan” by Kimura et al.

--Manuscript Draft--

<b>Manuscript Number:</b>							
<b>Full Title:</b>	Comment on “Earthquake-induced prompt gravity signals identified in dense array data in Japan” by Kimura et al.						
<b>Article Type:</b>	Comment						
<b>Section/Category:</b>	Seismology						
<b>Funding Information:</b>	<table border="1"><tr><td>Agence Nationale de la Recherche (ANR-14-CE03-0014-01)</td><td>Not applicable</td></tr><tr><td>Labex UnivEarthS (ANR-10-LABX-0023)</td><td>Not applicable</td></tr><tr><td>Labex UnivEarthS (ANR-11-IDEX-0005-02)</td><td>Not applicable</td></tr></table>	Agence Nationale de la Recherche (ANR-14-CE03-0014-01)	Not applicable	Labex UnivEarthS (ANR-10-LABX-0023)	Not applicable	Labex UnivEarthS (ANR-11-IDEX-0005-02)	Not applicable
Agence Nationale de la Recherche (ANR-14-CE03-0014-01)	Not applicable						
Labex UnivEarthS (ANR-10-LABX-0023)	Not applicable						
Labex UnivEarthS (ANR-11-IDEX-0005-02)	Not applicable						
<b>Abstract:</b>	<p>A recent work by Kimura et al. (2019) (hereafter referred to as K19) claims to provide the first observational constraints on the prompt elastogravity signals (PEGS) induced by an earthquake. To make their claim, the authors argue that the observations shown in Vallée et al. (2017) (hereafter referred to as V17) are spurious and their modeling inaccurate. Here we show that K19’s claim is invalid because it is based on flawed data processing. In fact, K19’s analysis involves an incomplete correction of the instrument response of broadband seismic sensors, which essentially dismisses low-frequency components of the data that are critical for the detection of intrinsically low-frequency signals such as PEGS. As a direct consequence, signals are much more difficult to observe than in V17, where the low part of the signal spectrum is carefully taken into account. This deficient data processing also explains why the signal amplitude reported by K19 after stacking data from multiple stations is lower than the individual signals reported by V17. Moreover, failing to take appropriate measures of data quality control, K19 used signals from low-quality sensors to call into question the signals detected by high-quality sensors. Finally, K19 use an inadequate simulation approach to model PEGS, in which the important effect of the ground acceleration induced by gravity changes is ignored. In summary, K19 do not show any viable arguments to question the observations and modeling of PEGS presented in V17.</p>						
<b>Corresponding Author:</b>	Martin Vallée Institut de Physique du Globe de Paris Paris, FRANCE						
<b>Corresponding Author Secondary Information:</b>							
<b>Corresponding Author’s Institution:</b>	Institut de Physique du Globe de Paris						
<b>Corresponding Author’s Secondary Institution:</b>							
<b>First Author:</b>	Martin Vallée						
<b>First Author Secondary Information:</b>							
<b>Order of Authors:</b>	<table border="1"><tr><td>Martin Vallée</td></tr><tr><td>Jean Paul Ampuero</td></tr><tr><td>Kévin Juhel</td></tr><tr><td>Pascal Bernard</td></tr><tr><td>Jean-Paul Montagner</td></tr><tr><td>Matteo Barsuglia</td></tr></table>	Martin Vallée	Jean Paul Ampuero	Kévin Juhel	Pascal Bernard	Jean-Paul Montagner	Matteo Barsuglia
Martin Vallée							
Jean Paul Ampuero							
Kévin Juhel							
Pascal Bernard							
Jean-Paul Montagner							
Matteo Barsuglia							
<b>Order of Authors Secondary Information:</b>							

<b>Suggested Reviewers:</b>	Goran Ekström ekstrom@ideo.columbia.edu
	Richard Allen rallen@berkeley.edu
	Peter Shearer pshearer@ucsd.edu
	Barbara Romanowicz barbara.romanowicz@gmail.com
<b>Opposed Reviewers:</b>	
<b>Manuscript Classifications:</b>	20: Seismology; 20.020: Earthquake, Tsunami

[Click here to view linked References](#)

1  
2  
3  
4  
5  
6  
7  
8  
9  
10  
11  
12  
13  
14  
15  
16  
17  
18  
19  
20  
21  
22  
23  
24  
25  
26  
27  
28  
29  
30  
31  
32  
33  
34  
35  
36  
37  
38  
39  
40  
41  
42  
43  
44  
45  
46  
47  
48  
49  
50  
51  
52  
53  
54  
55  
56  
57  
58  
59  
60  
61  
62  
63  
64  
65

1 **Title : Comment on “Earthquake-induced prompt gravity signals**

2 **identified in dense array data in Japan” by Kimura et al.**

3 **Author #1:** Martin Vallée, Institut de Physique du Globe de Paris, Sorbonne Paris Cité,

4 Université Paris Diderot, CNRS, Paris, France ; vallee@ipgp.fr

5 **Author #2:** Jean Paul Ampuero, Université Côte d’Azur, IRD, CNRS, Observatoire de la

6 Côte d’Azur, Géoazur, Sophia Antipolis, France ; ampuero@geoazur.unice.fr

7 **Author #3:** Kévin Juhel, Institut de Physique du Globe de Paris, Sorbonne Paris Cité,

8 Université Paris Diderot, CNRS, Paris, France AND AstroParticule et Cosmologie,

9 Université Paris Diderot, CNRS/IN2P3, Sorbonne Paris Cité, France ; juhel@ipgp.fr

10 **Author #4:** Pascal Bernard, Institut de Physique du Globe de Paris, Sorbonne Paris Cité,

11 Université Paris Diderot, CNRS, Paris, France ; bernard@ipgp.fr

12 **Author #5:** Jean-Paul Montagner, Institut de Physique du Globe de Paris, Sorbonne Paris

13 Cité, Université Paris Diderot, CNRS, Paris, France ; jpm@ipgp.fr

14 **Author #6:** Matteo Barsuglia, AstroParticule et Cosmologie, Université Paris Diderot,

15 CNRS/IN2P3, Sorbonne Paris Cité, France; barsu@apc.in2p3.fr

16 **Corresponding author : Martin Vallée**

17

1  
2  
3  
4 18 **Abstract**  
5  
6

7 19 A recent work by Kimura et al. (2019) (hereafter referred to as K19) claims to provide  
8  
9  
10 20 the first observational constraints on the prompt elastogravity signals (PEGS) induced by  
11  
12  
13  
14 21 an earthquake. To make their claim, the authors argue that the observations shown in  
15  
16  
17 22 Vallée et al. (2017) (hereafter referred to as V17) are spurious and their modeling  
18  
19  
20  
21 23 inaccurate. Here we show that K19's claim is invalid because it is based on flawed data  
22  
23  
24 24 processing. In fact, K19's analysis involves an incomplete correction of the instrument  
25  
26  
27  
28 25 response of broadband seismic sensors, which essentially dismisses low-frequency  
29  
30  
31  
32 26 components of the data that are critical for the detection of intrinsically low-frequency  
33  
34  
35 27 signals such as PEGS. As a direct consequence, signals are much more difficult to observe  
36  
37  
38  
39 28 than in V17, where the low part of the signal spectrum is carefully taken into account.  
40  
41  
42 29 This deficient data processing also explains why the signal amplitude reported by K19  
43  
44  
45  
46 30 after stacking data from multiple stations is lower than the individual signals reported by  
47  
48  
49  
50 31 V17. Moreover, failing to take appropriate measures of data quality control, K19 used  
51  
52  
53 32 signals from low-quality sensors to call into question the signals detected by high-quality  
54  
55  
56 33 sensors. Finally, K19 use an inadequate simulation approach to model PEGS, in which  
57  
58  
59  
60  
61  
62  
63  
64  
65

1  
2  
3  
4  
5  
6  
7  
8  
9  
10  
11  
12  
13  
14  
15  
16  
17  
18  
19  
20  
21  
22  
23  
24  
25  
26  
27  
28  
29  
30  
31  
32  
33  
34  
35  
36  
37  
38  
39  
40  
41  
42  
43  
44  
45  
46  
47  
48  
49  
50  
51  
52  
53  
54  
55  
56  
57  
58  
59  
60  
61  
62  
63  
64  
65

34 the important effect of the ground acceleration induced by gravity changes is ignored. In

35 summary, K19 do not show any viable arguments to question the observations and

36 modeling of PEGS presented in V17.

37

38

39 **Keywords**

40 Prompt elastogravity signals, Tohoku earthquake, instrument response, noise levels

1  
2  
3  
4 41 **Main Text**  
5  
6

7 42 **Introduction**  
8  
9

10 43           The study of prompt elastogravity signals (PEGS) generated by earthquakes is  
11  
12  
13  
14 44 now becoming a mature research area. After the pioneering works in modeling (Harms et  
15  
16  
17 45 al. 2015; Harms 2016; Heaton 2017) and observation (Montagner et al. 2016), PEGS have  
18  
19  
20  
21 46 been directly observed, understood and modeled in the last two years (Vallée et al., 2017;  
22  
23  
24 47 Juhel et al., 2018; Juhel et al., 2019; Vallée and Juhel 2019). In particular, Vallée et al.  
25  
26  
27  
28 48 (2017) (hereafter referred to as V17) showed that the data from regional high-quality  
29  
30  
31  
32 49 broadband sensors recording the 2011 Tohoku earthquake exhibit the distinctive features  
33  
34  
35 50 of PEGS. A downward acceleration trend is clearly observed before the P waves arrival  
36  
37  
38  
39 51 (Fig. 1 of V17), and its shape and amplitude at each station is consistent with modeling  
40  
41  
42 52 that includes both the coseismic gravity perturbations and their induced elastic Earth  
43  
44  
45  
46 53 response (Fig. 3 of V17). Juhel et al. (2019) confirmed, with a normal-mode modeling  
47  
48  
49 54 approach, the accuracy of the results of V17. Finally, PEGS observation is not restricted  
50  
51  
52  
53 55 to earthquakes with magnitude larger than 9, as shown by recent observations made for  
54  
55  
56 56 earthquakes with magnitudes between 7.9 and 8.8 (Vallée and Juhel 2019).  
57  
58  
59  
60  
61  
62  
63  
64  
65

1  
2  
3 57 In this context, Kimura et al. (2019) (hereafter referred to as K19) reexamined  
4  
5  
6  
7 58 the data of the 2011 Tohoku earthquake and claimed, to our surprise, that their study  
8  
9  
10 59 "*provides the first constraint of prompt elastogravity signals by observation*". These  
11  
12  
13  
14 60 authors argued that observations made by V17 are not confirmed by analysis of data from  
15  
16  
17 61 neighboring stations and "*were only local noises*", "*outliers*", or artifacts due to signal  
18  
19  
20  
21 62 processing. Here, we will show that all the arguments of K19 against the soundness of  
22  
23  
24 63 the analysis by V17 and the claim of originality of PEGS observation made by K19 are  
25  
26  
27  
28 64 invalid. We will focus on showing the following:

- 31  
32 65 1. The reasons why K19 failed to confirm the observations by V17 are trivial  
33  
34  
35 66 (section "Biased observational analysis made by K19"). We show that the  
36  
37  
38  
39 67 data processing used by K19 involves an incomplete correction for  
40  
41  
42 68 instrument response that de-emphasizes the low-frequency components of  
43  
44  
45 69 the data. However, PEGS are intrinsically low-frequency signals. The very  
46  
47  
48  
49 70 clear signals shown by V17 are weaker or even unobservable in the analysis  
50  
51  
52  
53 71 of K19 because the latter did not consider a suitable frequency band. In this  
54  
55  
56 72 section, we will also demonstrate the robustness of the V17 data processing.  
57  
58  
59  
60  
61  
62  
63  
64  
65

- 1  
2  
3 73 2. In addition to their inappropriate data processing, K19 do not take into  
4  
5  
6  
7 74 account station quality, and erroneously discard high-quality signals on the  
8  
9  
10 75 basis of noisy signals from neighboring stations. If K19 had used  
11  
12  
13  
14 76 appropriate data processing and quality control criteria, their study would  
15  
16  
17 77 have simply confirmed the V17 observations.  
18  
19  
20  
21 78 3. The claims of originality by K19 are invalid because they are based on  
22  
23  
24 79 inappropriate data processing. Failing to detect PEGS on data from  
25  
26  
27  
28 80 individual stations (with incorrect processing), K19 showed that PEGS are  
29  
30  
31  
32 81 detected after stacking data from multiple stations. But by doing so, the  
33  
34  
35 82 detection significance of their stack remains lower than even only one of  
36  
37  
38  
39 83 the individual signals shown in V17. Based on this stacking of incorrectly  
40  
41  
42 84 processed data, K19 incorrectly claimed their result provides the first  
43  
44  
45  
46 85 reliable PEGS observation.  
47  
48  
49 86 4. Inappropriate data processing also misled K19 into questioning the PEGS  
50  
51  
52  
53 87 modeling made in V17. The argument put forward by K19 is that the  
54  
55  
56 88 amplitude of their stack (of incorrectly processed data) is smaller than the  
57  
58  
59  
60  
61  
62  
63  
64  
65



1  
2  
3  
4  
5  
6  
7  
8  
9  
10  
11  
12  
13  
14  
15  
16  
17  
18  
19  
20  
21  
22  
23  
24  
25  
26  
27  
28  
29  
30  
31  
32  
33  
34  
35  
36  
37  
38  
39  
40  
41  
42  
43  
44  
45  
46  
47  
48  
49  
50  
51  
52  
53  
54  
55  
56  
57  
58  
59  
60  
61  
62  
63  
64  
65

89 signals observed and modeled by V17. We will show (in the "Erroneous  
90 conclusions about PEGS amplitudes" section) that stacking the same data  
91 as K19, but after instrument response correction following V17's procedure,  
92 results in a signal stack with the same amplitude as predicted by V17's  
93 model and with a much higher significance than K19's sub-optimal stack.

94

## 95 **Biased observational analysis made by K19**

### 96 **Inappropriate data processing with incomplete instrument response correction**

97 K19 used the following data pre-processing steps: (1) raw data were divided by  
98 the sensitivity coefficient of the broadband seismometers, which is defined as the  
99 velocity-to-counts conversion factor in the frequency band where the instrument response  
100 is flat, and (2) the result was converted into acceleration by differentiation. The  
101 frequency-independent conversion factor applied in step 1 is adequate for signals whose  
102 frequencies of interest are between a few 0.01 Hz to ~10 Hz, but is insufficient for PEGS  
103 observation. As shown in the theoretical study of Harms et al. (2015), the accelerations  
104 in PEGS are related to the second time integral of the seismic moment function, thus their

1  
2  
3 105 spectrum behaves as  $1/f^3$  at frequencies  $f$  lower than the earthquake corner frequency.  
4  
5

6  
7 106 PEGS are therefore low-frequency signals, and the potential to observe them with  
8  
9

10 107 seismometers is maximized when the lowest reliable frequencies are fully used. That is  
11  
12

13  
14 108 why V17 deconvolved the raw data by the instrument response, and carefully used a  
15  
16

17 109 causal high-pass filter at 0.002 Hz to mitigate the instrumental noise at even lower  
18  
19

20  
21 110 frequencies.  
22  
23

24 111 Figure 1 shows how much of the low-frequency signal in the analysis frequency  
25  
26

27  
28 112 band (0.002-0.03 Hz) is damped by the K19 processing compared to the V17 processing.  
29  
30

31 113 The low-frequency signal loss induced by the K19 processing is very large for STS2  
32  
33

34  
35 114 sensors (more than a factor of 15 of reduction at 0.002 Hz), and is significant even for  
36  
37

38 115 STS1 sensors (a factor larger than 2 at 0.002 Hz). Importantly, although it is not  
39  
40

41  
42 116 highlighted in K19 study, most of the sensors they used (9 out of 11 stations shown in  
43  
44

45  
46 117 their Figure 2 and 22 out of the 27 sensors used in their stacking analysis) are STS2  
47  
48

49 118 sensors. Not surprisingly, the only two sensors in which a signal is visible in their Figure  
50  
51

52  
53 119 2, FUK and SBR, are the STS1 sensors.  
54  
55

56 120 It is therefore obvious that the K19 processing lowers the PEGS detection  
57  
58  
59  
60  
61  
62  
63  
64  
65

1  
2  
3  
4  
5  
6  
7  
8  
9  
10  
11  
12  
13  
14  
15  
16  
17  
18  
19  
20  
21  
22  
23  
24  
25  
26  
27  
28  
29  
30  
31  
32  
33  
34  
35  
36  
37  
38  
39  
40  
41  
42  
43  
44  
45  
46  
47  
48  
49  
50  
51  
52  
53  
54  
55  
56  
57  
58  
59  
60  
61  
62  
63  
64  
65

121 potential but it is much less clear why they used such an observational strategy. K19  
122 justify their processing strategy as a way to avoid the non-causality of the instrument  
123 response deconvolution. Such a non-causality effect indeed exists, but is a problem only  
124 if the deconvolution is applied to a time series containing an undesirable subsequent  
125 signal. That is why it is crucial to cut the signals at the P-wave arrival, as done in the V17  
126 procedure, to avoid any contamination. Once this operation is done, it is difficult to  
127 imagine how a signal removed from the analysis (i.e. the P direct wave) could still have  
128 an adverse role. As K19 possibly worried about an influence of the limits of the original  
129 time windows, we show in Figure 2 that their arbitrary choice does not have any role on  
130 the obtained accelerations: as long as a sufficiently long pre-origin time signal is used and  
131 the P wave is not included, the V17 procedure gives the same acceleration signals in the  
132 0.002-0.03 Hz frequency range regardless of the choice of time window. We also recall  
133 that V17 provided in their Supplementary Material (Additional data) their exact data  
134 processing procedure (using Seismic Analysis Code – SAC), so that every reader can  
135 assess its robustness.

136           The V17 procedure is not affected by spurious effects and restores the signal

1  
2  
3 137 with higher fidelity than the K19 procedure. Thus any claim of non-detection using the  
4  
5  
6  
7 138 K19 procedure is highly dubious, especially if the signals are readily apparent with the  
8  
9  
10 139 V17 approach. For instance, at station NE93, K19 consider the signal (see their Fig. 3b)  
11  
12  
13  
14 140 as noise whereas V17 observe a signal with amplitude  $\sim 1$  nm/s<sup>2</sup>. NE93 is equipped with  
15  
16  
17 141 a CMG3T sensor, a broadband sensor with a response similar to that of an STS2, thus the  
18  
19  
20  
21 142 K19 procedure eliminates a large part of the PEGS recorded at this station.  
22  
23

24  
25 143

26  
27  
28 144 **Mixing high-quality with low-quality sensors**  
29  
30

31  
32 145 PEGS are not equally well recorded by all sensors, because of their intrinsic  
33  
34  
35 146 characteristics combined with differences in site quality. However, K19 used in their Figs.  
36  
37  
38  
39 147 2 and 3 all the existing broadband sensors in a given area, regardless of their quality, as  
40  
41  
42 148 an argument to discard the direct PEGS observations. They made the same error when  
43  
44  
45  
46 149 they directly compared the signals recorded by the Matsuhira gravimeter and by the  
47  
48  
49  
50 150 collocated MAJO seismometer, without acknowledging that the pre-event seismic noise  
51  
52  
53 151 at MAJO is much lower (see V17). Their Figs. 3a and 3b are also particularly misleading  
54  
55  
56 152 because signals are not shown with the same vertical scale. Finally, in Fig. 3a of K19,  
57  
58  
59  
60  
61  
62  
63  
64  
65

1  
2  
3 153 despite the deficient data processing, a signal is still visible at the excellent STS1 sensor  
4  
5  
6  
7 154 of station MDJ. K19 reject this evidence by judging it is inconsistent with data at  
8  
9  
10 155 neighboring stations. However, the difference is simply explained by the much lower  
11  
12  
13  
14 156 noise at MDJ.

15  
16  
17 157 In contrast, the V17 study considered all the signals that satisfy an objective  
18  
19  
20  
21 158 quality control criterion: their amplitude in the 1800 s preceding the earthquake had to be  
22  
23  
24 159 below a given amplitude threshold. This threshold was set at +/- 0.8 nm/s<sup>2</sup> so that a signal  
25  
26  
27  
28 160 with an amplitude of -1 nm/s<sup>2</sup> occurring just before the P arrival time is unlikely to be  
29  
30  
31  
32 161 random noise. All the sensors shown in Fig. 3 of K19, except for the NE93 and MDJ  
33  
34  
35 162 sensors used by V17, have pre-event noise amplitude levels of more than +/- 2 nm/s<sup>2</sup>, and  
36  
37  
38  
39 163 often much more. Such noisy data were not shown in the V17 study and they are of little  
40  
41  
42 164 use to invalidate PEGS observations.

43  
44  
45 165 At this stage, it is interesting to mention a specific point about the MDJ station.  
46  
47  
48  
49 166 If K19 had used the V17 data processing, they would have obtained the clear MDJ signals  
50  
51  
52  
53 167 that can be seen in Figs. 1, 2 and 3 of V17. When quantified by the Signal-to-Noise Ratio  
54  
55  
56 168 (SNR) criterion that K19 used to evaluate the stack significance (i.e. the ratio between  
57  
58  
59  
60  
61  
62  
63  
64  
65

1  
2  
3  
4  
5  
6  
7  
8  
9  
10  
11  
12  
13  
14  
15  
16  
17  
18  
19  
20  
21  
22  
23  
24  
25  
26  
27  
28  
29  
30  
31  
32  
33  
34  
35  
36  
37  
38  
39  
40  
41  
42  
43  
44  
45  
46  
47  
48  
49  
50  
51  
52  
53  
54  
55  
56  
57  
58  
59  
60  
61  
62  
63  
64  
65

169 the amplitude at the P arrival time and the standard deviation  $\sigma$  of the seismic noise), the  
170 SNR reaches  $\sim 9$  at station MDJ. When properly processed, this unique sensor has a better  
171 SNR than the stack of 27 stations considered by K19, whose SNR is only 7. The V17  
172 study did not require any stacking because it was based on signals that could be directly  
173 observed at several stations (and confirmed by signal modeling).

174

175 **Objective comparisons confirm V17 observations**

176           Based on the aforementioned considerations, Figs. 2 and 3 of K19 do not bring  
177 any valid argument to question the observations made by V17. On the contrary, the  
178 sensors in Southwest Japan used in Fig. 2 of K19 confirm the V17 observations. Some of  
179 these sensors, in addition to FUK also used in V17, indeed meet the pre-event noise  
180 quality criterion required by V17. This is expected because V17 explicitly mentioned that,  
181 to avoid redundant signals at similar locations, not all the high-quality F-net sensors were  
182 used in their analysis.

183           In practice, after application of the V17 data processing, four stations (FUK,  
184 SBR, IZH and INN) have pre-event noise whose absolute values remain below  $0.8 \text{ nm/s}^2$ ,

1  
2  
3 185 and therefore offer an unbiased opportunity to validate the FUK observations shown in  
4  
5  
6  
7 186 V17. Not surprisingly, these four signals, shown in Figure 3, strongly support the FUK  
8  
9  
10 187 observations: they all exhibit a clear downward trend after the earthquake origin time  
11  
12  
13  
14 188 (with an optimal SNR at the STS1 sensors FUK and SBR), with consistent amplitudes  
15  
16  
17 189 reaching values of  $\sim -1 \text{ nm/s}^2$  at the P arrival time.  
18  
19  
20

21 190

## 24 191 **Erroneous conclusions about signal amplitudes**

27 192 The K19 study does not provide any valid modeling of the expected PEGS  
28  
29  
30  
31 193 amplitudes. Although, based on the works of Heaton (2017) and V17, K19 correctly  
32  
33  
34  
35 194 described that PEGS originate from two effects, a direct gravity perturbation and an  
36  
37  
38  
39 195 induced ground acceleration, they only modelled the first effect. In their Fig. 1, K19 only  
40  
41  
42 196 show the direct gravity term, in the very crude approximation of an infinite space. The  
43  
44  
45  
46 197 values shown in their Fig. 1 differ by a factor of  $\sim 100$  compared to the amplitudes of their  
47  
48  
49 198 stack (their Fig. 7a), but K19 did not comment on why it is so.  
50  
51

52 199 Despite being unable to model their own observations, K19 try to discard the  
53  
54  
55  
56 200 modeling made by V17. While K19 correctly noted that the signal simulated by V17 was  
57  
58  
59  
60  
61  
62  
63  
64  
65

1  
2  
3  
4  
5  
6  
7  
8  
9  
10  
11  
12  
13  
14  
15  
16  
17  
18  
19  
20  
21  
22  
23  
24  
25  
26  
27  
28  
29  
30  
31  
32  
33  
34  
35  
36  
37  
38  
39  
40  
41  
42  
43  
44  
45  
46  
47  
48  
49  
50  
51  
52  
53  
54  
55  
56  
57  
58  
59  
60  
61  
62  
63  
64  
65

201 on the order of  $-1 \text{ nm/s}^2$ , they compared these amplitudes obtained in the 0.002-0.03 Hz  
202 frequency band with their observed stack amplitude ( $-0.25 \text{ nm/s}^2$ ), which suffers from  
203 strong deficit in this frequency band (Figure 1 and previous sections). K19 therefore  
204 appear unaware that meaningful comparisons between two signals can only be done if  
205 they have been processed in the same way.

206 Observations and theory are fortunately in much better agreement when  
207 comparisons are properly made in the same frequency band. In Figure 4, we show the  
208 stacked trace of the same 27 stations used by K19, but applying the instrument response  
209 correction used by V17. The observed stack amplitude confirms that the PEGS in  
210 Southwest Japan in the 0.002-0.03 Hz frequency band reach an amplitude of the order of  
211  $-1 \text{ nm/s}^2$  at the P-wave arrival time, consistently with the V17 modeling. Moreover, the  
212 SNR of the stack reaches a value of 14 with the V17 processing, whereas K19 obtained a  
213 smaller value of 7 with their processing. Thus, the appropriate data processing strongly  
214 increases the significance of the stack. In more challenging observation configurations  
215 than the Tohoku earthquake case, this difference is clearly key for PEGS detection.

216 Contrary to the opinion expressed by K19, there is no urgent need to improve



1  
2  
3 217 the V17 modeling approach and to develop a “*better theoretical model [...] that addresses*  
4  
5  
6 218 *the fully coupled equations between the elastic deformation and gravity*”. The adequacy  
7  
8  
9  
10 219 of the V17 and Juhel et al. (2019) approaches is not only supported by their agreement  
11  
12  
13  
14 220 with the observations: V17 showed that the error made by neglecting the full coupling  
15  
16  
17 221 (i.e. by neglecting that gravity-induced motion itself creates a gravity perturbation, and  
18  
19  
20  
21 222 so on) is only a few percent. Additionally, Juhel et al. (2019) numerically modeled the  
22  
23  
24 223 direct gravity perturbation with and without self-gravitation and found only minor  
25  
26  
27  
28 224 differences in the 0.002-0.03 Hz frequency band of interest. Solving the fully coupled  
29  
30  
31  
32 225 equations is therefore a numerical challenge that would offer a more elegant solution, but  
33  
34  
35 226 is not a prerequisite to model the PEGS observations.  
36  
37

38 227  
39  
40

## 41 42 228 **Conclusion** 43 44

45 229 K19’s study illustrates the difficulties to observe a small-amplitude signal when  
46  
47  
48  
49 230 using non-optimal data processing or non-optimal sensors. This trivial finding does not  
50  
51  
52  
53 231 provide any valid argument to challenge previous observations made by V17 using a  
54  
55  
56 232 better processing applied to objectively selected data. K19’s claims to discard previous  
57  
58  
59  
60  
61  
62  
63  
64  
65

1  
2  
3  
4  
5  
6  
7  
8  
9  
10  
11  
12  
13  
14  
15  
16  
17  
18  
19  
20  
21  
22  
23  
24  
25  
26  
27  
28  
29  
30  
31  
32  
33  
34  
35  
36  
37  
38  
39  
40  
41  
42  
43  
44  
45  
46  
47  
48  
49  
50  
51  
52  
53  
54  
55  
56  
57  
58  
59  
60  
61  
62  
63  
64  
65

233 PEGS modeling is based on an obviously biased use of their observations. In light of  
234 these two major errors, their claims of pioneering findings are invalid.

235           The K19 study provides only a modest contribution to the recent PEGS  
236 observations made by other groups, and in particular by the V17 study. Recent progress  
237 in the research on PEGS has yielded new advances that go far beyond the K19 study.  
238 Readers interested in how PEGS can be optimally observed may refer to the more  
239 sophisticated stacking approaches described by Montagner et al. (2016) and Vallée and  
240 Juhel (2019). Vallée and Juhel (2019) also show how multiple PEGS observations made  
241 for earthquakes of different focal mechanisms and depths are accurately modeled by the  
242 methods described by V17 and Juhel et al. (2019). Therefore, the remaining challenges  
243 today are no longer to show that PEGS are well understood, modeled, and observed for  
244 magnitudes larger than 8, but to lower this magnitude threshold and to reduce the  
245 detection delay, in order to make PEGS even more valuable for early warning systems.

246  
247

1  
2  
3  
4  
5  
6  
7  
8  
9  
10  
11  
12  
13  
14  
15  
16  
17  
18  
19  
20  
21  
22  
23  
24  
25  
26  
27  
28  
29  
30  
31  
32  
33  
34  
35  
36  
37  
38  
39  
40  
41  
42  
43  
44  
45  
46  
47  
48  
49  
50  
51  
52  
53  
54  
55  
56  
57  
58  
59  
60  
61  
62  
63  
64  
65

248 **Declarations**

249 **Ethics approval and consent to participate**

250 Not applicable

251 **Consent for publication**

252 Not applicable

253 **List of abbreviations**

254 FUK: Fukue; F-net: Full range Seismograph Network of Japan; INN:

255 Nakatsu; IZH: Izuhara; K19: Kimura et al. (2019); MAJO: Matsuhira;

256 MDJ: Mudanjiang; NE93: Zhalaiteqi Badaerhuzhen; PEGS: Prompt

257 elastogravity signals; SAC: Seismic Analysis Code; SNR: Signal-To-

258 Noise; SBR : Sefuri; V17: Vallée et al. (2017)

259 **Availability of data and materials**

260 Data from the F-net network are publicly available at the NIED F-net

261 server: <http://www.fnet.bosai.go.jp>. MAJO station belongs to the GSN

262 network (<https://doi.org/10.7914/SN/IU>), MDJ station to the NCDSN

263 network (<https://doi.org/10.7914/SN/IC>), and NE93 to the NECESS/UT

1  
2  
3  
4  
5  
6  
7  
8  
9  
10  
11  
12  
13  
14  
15  
16  
17  
18  
19  
20  
21  
22  
23  
24  
25  
26  
27  
28  
29  
30  
31  
32  
33  
34  
35  
36  
37  
38  
39  
40  
41  
42  
43  
44  
45  
46  
47  
48  
49  
50  
51  
52  
53  
54  
55  
56  
57  
58  
59  
60  
61  
62  
63  
64  
65

264 network ([https://doi.org/10.7914/SN/YP\\_2009](https://doi.org/10.7914/SN/YP_2009)). Data from the GSN,  
265 NCDSN and NECESS/UT networks are publicly available at the IRIS data  
266 management center (<http://ds.iris.edu/ds/nodes/dmc/>).

**Competing interests**

The authors declare no competing interests.

**Funding**

We acknowledge the financial support from the UnivEarthS Labex program  
at Sorbonne Paris Cité (ANR-10-LABX-0023 and ANR-11-IDEX-0005-02)  
and from the Agence Nationale de la Recherche (grant ANR-14-CE03-0014-  
01)

**Authors' contributions**

MV designed this comment, with inputs from KJ and JPA. MV performed  
the data analysis, produced the associated figures, and wrote the text with  
JPA. KJ, JPM, MB and PB commented the initial versions of the manuscript.

**Acknowledgments**

The SAC (<http://ds.iris.edu/ds/nodes/dmc/software/downloads/sac/>) free

1  
2  
3 280 software was used for data processing. Most numerical computations were

4  
5  
6  
7 281 performed on the S-CAPAD platform, Paris, France.

8  
9  
10 282

11  
12  
13  
14 283 **References**

15  
16  
17 284 Harms, J. (2016) Transient gravity perturbations from a double-couple in a homogeneous

18  
19  
20  
21 285 half-space, *Geophys J Int* 205:1153–1164. doi: 10.1093/gji/ggw076

22  
23  
24 286 Harms, J., Ampuero, J.-P., Barsuglia, M., Chassande-Mottin, E., Montagner, J.-P.,

25  
26  
27  
28 287 Somala, S.N., Whiting, B.F. (2015) Transient gravity perturbations induced by

29  
30  
31 288 earthquake rupture. *Geophys J Int* 201:1416–1425. doi: 10.1093/gji/ggv090

32  
33  
34  
35 289 Heaton, T. H. (2017) Correspondence: response of a gravimeter to an instantaneous step

36  
37  
38 290 in gravity. *Nat Commun.* 8:966. doi:10.1038/s41467-01701348-z.

39  
40  
41  
42 291 Kimura, M., Kame, N., Watada, S., Ohtani, M., Araya, A., Imanishi, Y., Ando, M.,

43  
44  
45 292 Kunugi, T. (2019) Earthquake-induced prompt gravity signals identified in dense

46  
47  
48  
49 293 array data in Japan. *Earth Planets Space* 71:27. doi:10.1186/s40623-019-1006-x

50  
51  
52  
53 294 Juhel, K., Ampuero, J. P., Barsuglia, M., Bernard, P., Chassande-Mottin, E., Fiorucci, D.,

54  
55  
56 295 Harms, J., Montagner, J.-P, Vallée, M., Whiting, B. F. (2018) Earthquake early

1  
2  
3  
4  
5  
6  
7  
8  
9  
10  
11  
12  
13  
14  
15  
16  
17  
18  
19  
20  
21  
22  
23  
24  
25  
26  
27  
28  
29  
30  
31  
32  
33  
34  
35  
36  
37  
38  
39  
40  
41  
42  
43  
44  
45  
46  
47  
48  
49  
50  
51  
52  
53  
54  
55  
56  
57  
58  
59  
60  
61  
62  
63  
64  
65

296 warning using future generation gravity strainmeters. *J Geophys Res* 123:10,889-  
297 10,902. doi: 10.1029/2018JB016698

298 Juhel, K., Montagner, J.-P., Vallée, M., Ampuero, J. P., Barsuglia, M., Bernard, P.,  
299 Clévéde, E., Harms, J., Whiting, B. F. (2019) Normal mode simulation of prompt  
300 elastogravity signals induced by an earthquake rupture *Geophys J Int* 216:935-947.  
301 doi: 10.1093/gji/ggy436

302 Montagner, J.-P., Juhel, K., Barsuglia, M., Ampuero, J. P., Chassande-Mottin, E., Harms,  
303 J., Whiting, B.F., Bernard, P., Clévéde, E., Lognonné, P. (2016) Prompt gravity  
304 signal induced by the 2011 Tohoku-Oki earthquake. *Nat Commun* 7:13349,  
305 doi:10.1038/ncomms13349

306 Vallée, M., Ampuero, J. P., Juhel, K., Bernard, P., Montagner, J.-P., Barsuglia, M. (2017)  
307 Observations and modeling of the elastogravity signals preceding direct seismic  
308 waves. *Science* 358:1164-1168. doi: 10.1126/science.aao0746

309 Vallée, M., Juhel, K. (2019) Multiple observations of the prompt elastogravity signals  
310 heralding direct seismic waves. *J Geophys Res*. doi: 10.1029/2018JB017130

1  
2  
3  
4  
5  
6  
7  
8  
9  
10  
11  
12  
13  
14  
15  
16  
17  
18  
19  
20  
21  
22  
23  
24  
25  
26  
27  
28  
29  
30  
31  
32  
33  
34  
35  
36  
37  
38  
39  
40  
41  
42  
43  
44  
45  
46  
47  
48  
49  
50  
51  
52  
53  
54  
55  
56  
57  
58  
59  
60  
61  
62  
63  
64  
65

311 **Figure legends**

312

313 **Figure 1** : Low-frequency deficit induced by the instrument correction made by K19.

314 Black lines show how an acceleration signal with flat spectrum is recorded by several

315 sensors as a function of frequency (modified from Fig. S1 of K19). The V17 correction

316 uses the complete instrument response of the STS1 and STS2 sensors (dashed and dotted

317 lines, respectively) while the K19 correction uses a frequency-independent counts-to-

318 velocity conversion factor (blue and red lines, respectively). The blue and red areas (for

319 STS1 and STS2, respectively) highlight the difference between the two procedures in the

320 analyzed frequency range, 0.002-0.03 Hz.

321

322 **Figure 2** : Robustness of the V17 data processing illustrated for two stations of the F-net

323 network. FUK (top) and INN (bottom) are STS1 and STS2 sensors, respectively. For each

324 sensor, the curves show the obtained vertical acceleration signals for different choices of

325 the original time window. These choices can be read in the name given to each curve: the

326 negative number following “OT” gives the starting time (in s) of the window relative to

1  
2  
3 327 the Tohoku earthquake origin time; the negative number following “TP” gives the ending  
4  
5  
6  
7 328 time (in s) of the window relative to the P wave arrival time at each station. No differences  
8  
9  
10 329 can be observed in the resulting accelerations in the 0.002 - 0.03 Hz frequency band.

11  
12  
13  
14 330

15  
16  
17 331 **Figure 3** : Objective comparison between PEGS signals observed in Southwest Japan.

18  
19  
20  
21 332 All signals have been processed using the V17 procedure and the FUK signal (top row)

22  
23  
24 333 is therefore exactly the same as the one shown in Figs. 1 and 3 of V17. The other three

25  
26  
27  
28 334 signals are the only other ones among the stations shown in Fig. 2 of K19 that meet the

29  
30  
31 335 quality criterion of V17. All signals show consistent PEGS, supporting the use of only

32  
33  
34  
35 336 one of them (FUK) in the V17 study. Due to its correct data processing and appropriate

36  
37  
38  
39 337 noise considerations, this figure is the logical alternative to Fig. 2b of K19.

40  
41  
42 338

43  
44  
45 339 **Figure 4** : Consistency between observed PEGS amplitudes and V17 modeling. Stacked

46  
47  
48  
49 340 trace (station-averaged vertical acceleration) of the same 27 sensors considered in Fig. 7a

50  
51  
52  
53 341 of K19, but deconvolving the data by the instrument response (as done in V17) before

54  
55  
56 342 stacking. Note that the stacked trace  $S_s$  is shown with an opposite sign (scale to the right).

57  
58  
59  
60  
61  
62  
63  
64  
65



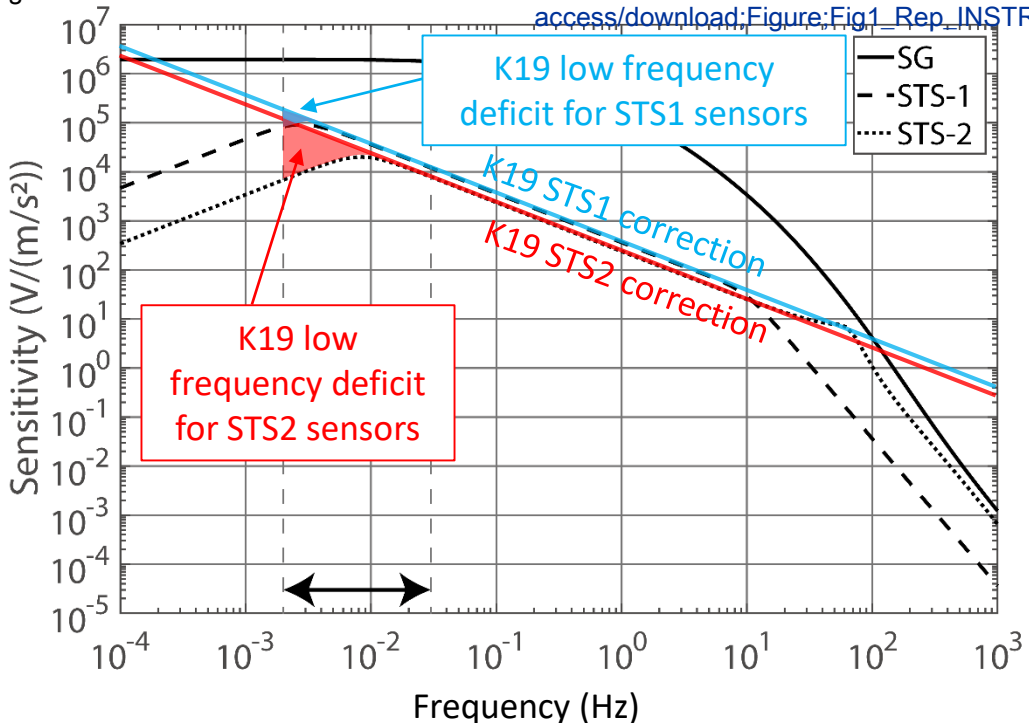
1  
2  
3  
4  
5  
6  
7  
8  
9  
10  
11  
12  
13  
14  
15  
16  
17  
18  
19  
20  
21  
22  
23  
24  
25  
26  
27  
28  
29  
30  
31  
32  
33  
34  
35  
36  
37  
38  
39  
40  
41  
42  
43  
44  
45  
46  
47  
48  
49  
50  
51  
52  
53  
54  
55  
56  
57  
58  
59  
60  
61  
62  
63  
64  
65

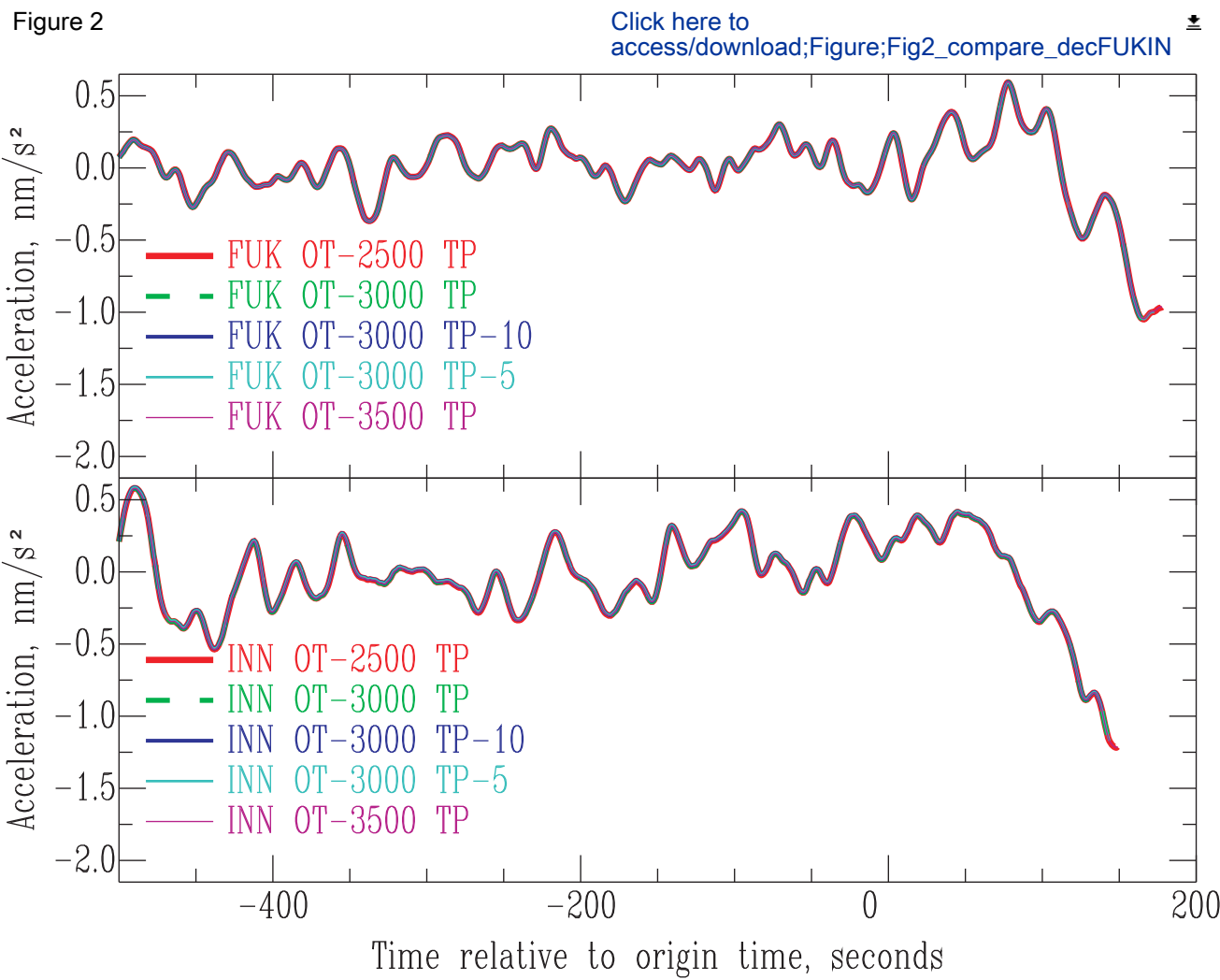
343 The stack SNR (scale to the left) is defined as the ratio between  $|S_s|$  and the standard  
344 deviation of noise calculated in the 10 minutes preceding earthquake origin time. At the  
345 P wave arrival,  $S_s \sim -1 \text{ nm/s}^2$  and SNR  $\sim 14$ .

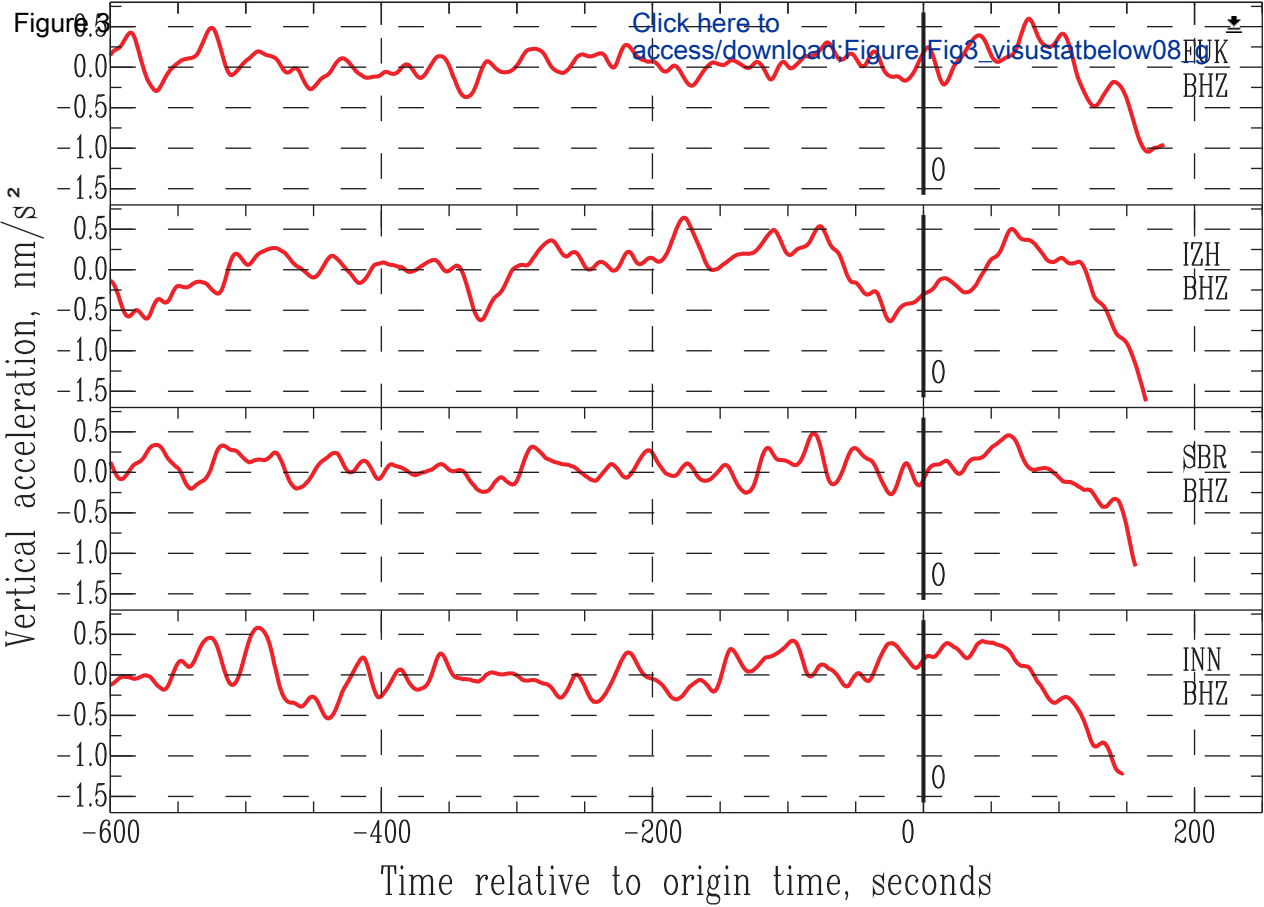
346

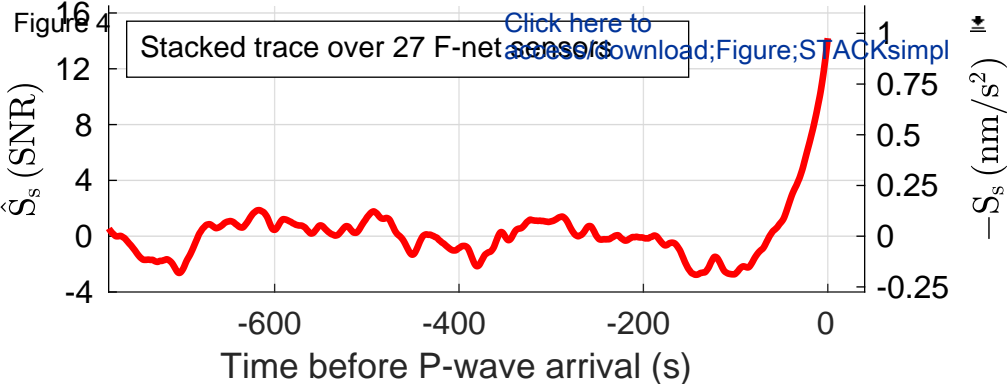
Figure 1

[Click here to access/download;Figure;Fig1\\_Rep\\_INSTR](#)









## Prompt elastogravity signals recorded by the high-quality seismic sensors in Southwest Japan confirm previous observations and modeling

